EurJIC European Journal of Inorganic Chemistry

ChemPubSoc Europe

FULL PAPER

DOI:10.1002/ejic.201301225

Ruthenium–Nitrosyl Complexes Derived from Ligands Containing Two Carboxylate Functional Groups and Studies on the Photolability of Coordinated NO

Kaushik Ghosh,*[a] Sushil Kumar,[a] and Rajan Kumar[a]

Ruthenium / NO ligand / Nitric oxide / Photochemistry / Quenching

Ruthenium complexes $[Ru^{III}(L^1)(PPh_3)_2(Cl)]$ (**1**) and $[Ru^{III}(L^2)(PPh_3)_2(Cl)]$ (**2**) (in which L^1H_2 and L^2H_2 are iminodiacetic acid and pyridine-2,6-dicarboxylic acid, respectively, and H stands for a dissociable proton) derived from the ligands that contain two carboxylate groups were synthesized and characterized. These complexes were treated with in situ generated NO derived from acidified nitrite solution, which afforded the formation of two $\{Ru–NO\}^6$ complexes $[Ru(L^1)(PPh_3)_2(NO)](ClO_4)$ (**1a**) and $[Ru(L^2)(PPh_3)_2(NO)](ClO_4)$ (**2a**). The molecular structure of the representative complex $[Ru(L^2)(PPh_3)_2(NO)](ClO_4)$ (**2a**) was determined using X-ray crystallography. Characterization of complexes **1a** and **2a** by IR and NMR spectroscopic studies revealed the presence of $\{Ru–NO\}^6$ species with $S = 0$ ground state. ESI-MS data also supported the formation of **1a** and **2a**. Exposure to UV light promoted rapid loss of NO from both ruthenium nitrosyls to generate Ru^{III} photoproducts of the type $[Ru(L)(PPh_3)_2(S)](ClO_4)$ (in which S stands for solvent). The quantum yields of NO photorelease for complexes **1a** and **2a** were measured using a chemical actinometry study. The NO released in solution was estimated using the Griess reagent, and the results were compared with the data obtained from sodium nitroprusside (SNP). A 2,2-diphenyl-1-picrylhydrazine (DPPH) radical quenching assay was performed to estimate the amount of generated reactive nitrogen species and/or reactive oxygen species under aerobic conditions during photolysis of NO.

Introduction

Nitric oxide (NO) is a diatomic free-radical species and has been recognized as an important signaling molecule that plays important roles in different biological processes including blood-pressure regulation, neurotransmission, immune response, and cellular apoptosis.[1] In 1992, NO was voted the "molecule of the year" by *Science*,[2] and in 1998, the Nobel Prize was given to three US scientists, namely, Robert F. Furchgott, Louis J. Ignarro, and Ferid Murad in Stockholm, Sweden for their discovery of NO as a signaling molecule in biological systems. The biological activities of NO depend on the concentration of nitric oxide. In general, the low concentration of NO (nM to low μM) affects vasodilatation of smooth muscles and neurotransmission in the brain;[3] however, higher concentrations of NO (μM to mM) can lead to cell death.[4] During the past few years, there has been an upsurge of interest in the syntheses of metal–nitrosyl complexes for NO delivery by several groups.[5–9]

As part of our ongoing research, we reported the role of carbanion in the coordination and photolability of NO.[10] The carboxylate functional group is ubiquitous in biological molecules, and hence we are also trying to understand the role of carboxylate and carboxamide functional groups in these reactivity studies.[11–13] Herein, we report the synthesis and characterization of two structurally similar ruthenium–nitrosyl complexes, $[Ru(L^1)(PPh_3)_2(NO)](ClO_4)$ (**1a**) and $[Ru(L^2)(PPh_3)_2(NO)](ClO_4)$ (**2a**) (in which L^1H_2 and L^2H_2 are iminodiacetic acid and pyridine-2,6-dicarboxylic acid, respectively, and H stands for a dissociable proton; shown in Scheme 1). In our preliminary communication, the photolability studies of complex $[Ru(L^2)(PPh_3)_2(NO)](ClO_4)$ (**2a**) were described;[11] however, in the present report, we describe detailed studies on these complexes. The molecular structure of representative complex **2a** was determined by X-ray diffraction study. A few properties of the molecule will be discussed in light of DFT calculations. Bond lengths and bond angles obtained by means of X-ray crystallography and theoretical calculations were compared.

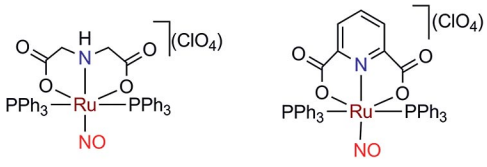

Scheme 1. Schematic drawings of nitrosyl complexes **1a** and **2a**.

[a] Department of Chemistry, Indian Institute of Technology, Roorkee,
Roorkee 247667, Uttarakhand, India
E-mail: ghoshfcy@iitr.ernet.in
http://www.iitr.ac.in

Supporting information for this article is available on the WWW under http://dx.doi.org/10.1002/ejic.201301225.

An estimation of the amount of photodissociated NO was also carried out using a Griess reagent assay. The amount of generated reactive nitrogen species and/or reactive oxygen species during photolysis of NO was determined by 2,2-diphenyl-1-picrylhydrazine (DPPH) radical quenching studies under aerobic conditions. The quantum yields of NO photorelease for complexes **1a** and **2a** were measured using a chemical actinometry study (ferrioxalate actinometer).

Results and Discussion

Synthesis

The precursor complexes $[Ru^{III}(L^1)(PPh_3)_2(Cl)]$ (**1**) and $[Ru^{III}(L^2)(PPh_3)_2(Cl)]$ (**2**) were synthesized by heating to reflux solutions of iminodiacetic acid and pyridine-2,6-dicarboxylic acid, respectively, in ethanol with $[Ru(PPh_3)_3Cl_2]$ in a 1:1 equivalent ratio. The brown-red complexes **1** and **2** were eluted through an alumina column and were recrystallized from a benzene/ethanol mixture (1:1 v/v). They were characterized by UV/Vis and IR spectral studies, which authenticated the formation of complexes **1** and **2**. These complexes were treated with in situ generated NO by an acidified (pH ≈ 2.3) sodium nitrite ($NaNO_2$) solution. To synthesize complex **1a**, a mixture of complex **1** and $NaNO_2$ was heated to reflux in methanol for an hour followed by acidification with perchloric acid ($HClO_4$). The color of **1** turned yellow within 15 minutes. The resultant yellow compound was nitrosyl complex $[Ru(L^1)(PPh_3)_2(NO)](ClO_4)$ (**1a**), isolated as a perchlorate salt. To obtain complex $[Ru(L^2)(PPh_3)_2(NO)](ClO_4)$ (**2a**), first acidified distill water was layered over a solution of **2** in dichloromethane, and then sodium nitrite was added. This bilayered mixture was stirred for 1.5 hours to obtain an orange-yellow solution of **2a**.[11] No change was observed when complexes **1** or **2** were treated with same acidic solution without $NaNO_2$. All the complexes were found to be soluble in most of the organic solvents such as dichloromethane, methanol, acetonitrile, and *N*,*N*′-dimethylformamide, but they were less soluble in water. The synthetic procedures for the complexes described above are summarized in Scheme 2.

Description of Structure

An ORTEP drawing of the representative complex $[Ru(L^2)(PPh_3)_2(NO)](ClO_4)$ (**2a**) is displayed in Figure 1. The selected bond lengths and bond angles for complex **2a**·CH_2Cl_2 are listed in Table 1, and the crystallographic matrix parameters are displayed below in Table 3. The crystal structure of **2a** afforded a tridentate coordination of li-

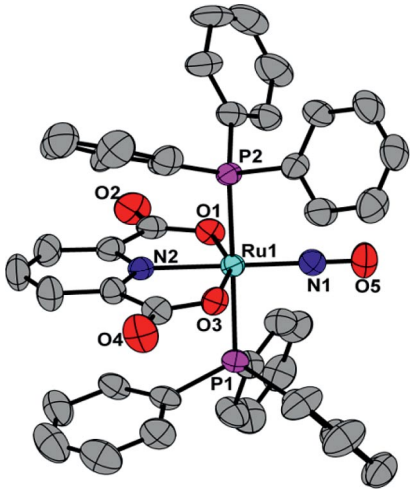

Figure 1. ORTEP diagram (50% probability level) of the cation of complex $[Ru(L^2)(PPh_3)_2(NO)](ClO_4)$ (**2a**). Hydrogen atoms and solvent molecules are not shown for clarity.

Table 1. Selected bond lengths [Å] and bond angles [°] for **2a**·CH_2Cl_2 along with the optimized DFT bond lengths and bond angles for comparison.

	X-ray	DFT
Bond lengths [Å]		
Ru1–O1	2.050(3)	2.092
Ru1–O3	2.065(3)	2.073
Ru1–P1	2.4606(13)	2.557
Ru1–P2	2.4576(13)	2.557
Ru1–N1	1.749(4)	1.782
Ru1–N2	2.017(4)	2.045
N1–O5	1.147(5)	1.188
Bond angles [°]		
Ru1–N1–O5	178.0(5)	178.61
N1–Ru1–N2	177.65(18)	178.13
N1–Ru1–P1	89.68(14)	90.39
N2–Ru1–P1	89.80(11)	89.70
O1–Ru1–P1	92.02(10)	87.12
O1–Ru1–N1	100.27(17)	104.78
O1–Ru1–N2	77.46(14)	77.08
O1–Ru1–O3	154.99(13)	154.69
N1–Ru1–O3	104.74(17)	100.52
P1–Ru1–P2	174.94(4)	174.20

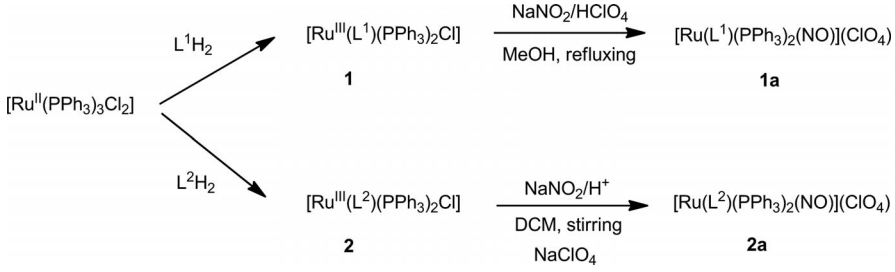

Scheme 2. Synthetic routes for complexes **1**, **2**, **1a**, and **2a**.

gand (L^2H_2), with one nitrogen atom (N2) and two carboxylato-O coordinated to the ruthenium center. The nitrosyl ligand (NO) was observed at the position *trans* to the pyridine nitrogen. The tridentate ligand and NO constituted the equatorial plane, and the axial positions were occupied by two phosphine groups. This coordination gave rise to distorted-octahedral geometry around the ruthenium center. The bond lengths of $Ru–O_{carboxylato}$,[13,14] Ru–P,[10,15–17] and $Ru–N_{py}$[18] were found to be consistent with the values reported in the literature.

In complex **2a**, the Ru1–N1–O5 bond angle and the Ru–N1(NO) and N1–O5 distances were found to be 178.0°, 1.749(4) Å, and 1.147(5) Å, respectively. These values were observed to be similar to the values available in the literature.[7d–7f,9c,9d,10,12,13] These data along with the ν_{NO} value at 1895 cm^{-1} (see below) clearly indicated the presence of the $\{Ru^{II}–NO^+\}^6$ moiety in the molecule. The back-bonding property of NO (π-acid ligand) was found to be dependent on other ligands present in the complex.

In fact, the structural parameters are dependent on the Ru–NO π interaction. In the ruthenium–nitrosyl complexes, the greater the Ru→NO back-bonding, the smaller the Ru–N–O angle and Ru–N(NO) distance. Consequently, the NO distance will be longer. The presence of other π-acid ligand(s) in the complex is an important factor in determining the values of the Ru–N–O angle as well as the Ru–N and N–O distances. Our data for complex **2a** are similar to the data reported by Mascharak and co-workers[7d,7e] and Lahiri and co-workers.[9c,9d] The extent of Ru→NO π-back-bonding for our complex (**2a**) is lower, probably owing to the presence of two phosphine and one pyridine ligands. The ligands described by Mascharak and co-workers[7d,7e] and the presence of the 2,2′;6′,2"-terpyridine (terpy) ligand in the complex reported by Lahiri and co-workers[9c,9d] gave rise to lesser Ru→NO π-back-bonding, and hence the reported data were similar to the data obtained by us.

The weak noncovalent interactions have many applications in the research area of nanoscience, materials chemistry, and biochemistry.[19] The noncovalent interactions found in the packing diagram of complex **2a**·CH_2Cl_2 are shown in Figure S1 of the Supporting Information. Oxygen atoms of perchlorate ion showed a weak hydrogen-bonding interaction (C–H···O interaction) with the aryl hydrogen of the phosphine [2.399(6) Å] group and with hydrogen atoms of the pyridine ring. A noncovalent interaction between the perchlorate oxygen and the crystallized dichloromethane molecule was also found, with a distance of 2.556(11) Å between them.

Spectral Studies

A peak near 1650 cm^{-1} was observed in the IR spectra of complexes **1** and **2**, which was assigned as a carbonyl stretching frequency (ν_{CO}) of carboxylate groups.[20] However, after nitrosylation, a higher shift of approximately 30 cm^{-1} in the ν_{CO} values was observed in complexes **1a** and **2a**. The IR spectra of **1a** and **2a** (shown in Figure S2 of the Supporting Information) provided ν_{NO} values near 1880 and 1895 cm^{-1}, respectively,[1d] and the presence of perchlorate ions was confirmed by the peaks near 1090 and 623 cm^{-1}.[10] The value of ν_{NO} near 1895 cm^{-1} in **2a** was found to be consistent with the data reported by Karidi et al.[21] and our previous reports[11] in which coordinated NO was *trans* to pyridine nitrogen donor. Hence we obtained the ruthenium–nitrosyl complexes with $\{Ru–NO\}^6$ moieties through the substitution of chloride ions by non-innocent NO ligand.[22] In all the complexes (**1**, **2**, **1a**, and **2a**), the bands near 746, 695, and 520 cm^{-1} indicated the presence of PPh_3 groups.[10,23–25]

An absorption band with λ_{max} near 458 and 400 nm was observed in the UV/Vis spectra of complexes **1** and **2**, respectively (Figure S3 in the Supporting Information). These absorptions were assigned to ligand-to-metal charge-transfer transitions. In the nitrosyl complex **1a**, only a peak near 280 nm was observed, and no peak was observed in the visible range. On the other hand, complex **2a** afforded a peak near 320 nm (Figure 2). Molar extinction coefficients (ε) of the band observed near 320 nm indicated metal-to-ligand charge-transfer (MLCT) transitions {Ru(d)→NO(π*) transitions}.[7d] Time-dependent density functional theoretical (TDDFT) calculations on **2a** also indicated the same (see below).

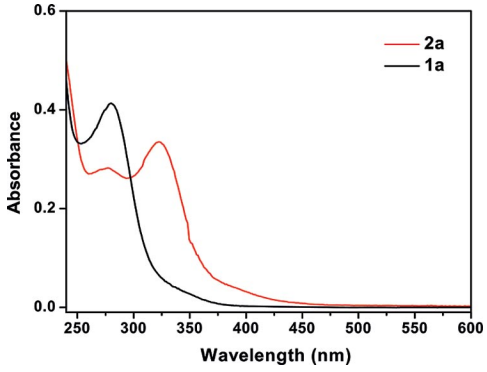

Figure 2. Electronic absorption spectra of complexes **1a** and **2a** in dichloromethane.

^1H and ^{31}P NMR spectra (solutions prepared and run under the dark conditions) clearly depicted the presence of the $S = 0$ ground state in nitrosyl complexes **1a** and **2a**.[10] ^1H NMR spectra of **1a** and **2a** clearly showed the presence of protons from carboxylate ligands and phosphine groups (Figures S4 and S5 in the Supporting Information). Moreover *trans* disposition of PPh_3 ligands was confirmed by single resonances near $\delta = 20.0$ ppm in the ^{31}P NMR spectra of both of the nitrosyl complexes (Figure S6 in the Supporting Information).[10,26]

We have investigated the ESI mass spectral studies for nitrosyl complexes **1a** and **2a**, and their experimental spectra along with the proposed fragmentation patterns are displayed in Figures S7 and S8, respectively, of the Supporting Information. The molecular ion peaks at m/z = 886.05 [M^+] for **1a** and at m/z = 919.5 [M^+] for **2a** were not detected in their ESI mass spectra; however, the most abundant peaks

at m/z = 786.9 $[M–ClO_4]^+$ and at m/z = 820.99 $[M–ClO_4]^+$, which correspond to the mono-positive complex cations, were found. These data clearly indicated the dissociation of perchlorate ions; however, all these data confirmed the formation of the nitrosyl complexes $[Ru(L^1)(PPh_3)_2(NO)](ClO_4)$ (**1a**) and $[Ru(L^2)(PPh_3)_2(NO)](ClO_4)$ (**2a**). In addition, the peak at m/z = 558.13 $[(M–ClO_4) – PPh_3]^+$ in the case of **2a** was probably due to the dissociation of one of the PPh_3 groups.

Photolysis Experiments: Estimation of Photoreleased NO

Complexes **1a** and **2a** were found to be photolabile, and the photolysis experiments of these nitrosyls were performed under visible as well as UV light. Exposure of an acetonitrile solution of **1a** (ca. 10^{-5} M) to low-intensity UV light (λ_{max} = 365 nm) causes the loss of NO (shown in Figure 3) with the disappearance of the peak near 282 nm. Spectral changes owing to light irradiation afforded two isosbestic points with λ_{max} near 250 and 355 nm. The photolability studies of complex **2a** were described in our previous report.[11]

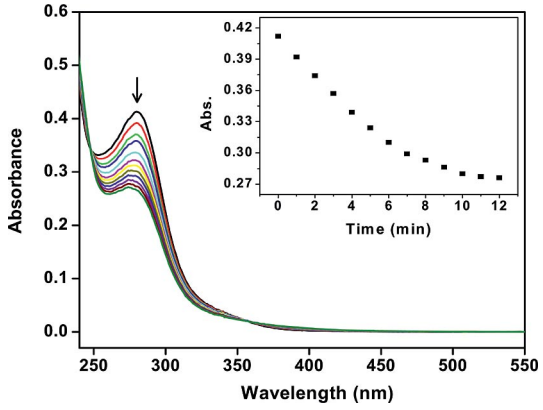

Figure 3. Photodissociation of NO from a solution of **1a** (ca. 1.6×10^{-5} M) in acetonitrile under illumination of a low-intensity UV lamp (λ_{max} = 365 nm). Repetitive scans were taken in 1 min intervals. Inset: Time-dependent changes in absorbance with λ_{max} near 282 nm at room temperature.

The quantum yield (ϕ) values for solutions of complexes **1a** and **2a** (λ_{irr} = 365 nm) were found to be 0.011 ± 0.001 and 0.012 ± 0.001, respectively, in dichloromethane, which showed that the NO-donating capacity of both the nitrosyl complexes was close to each other.[1d]

The amount of photoreleased NO from the nitrosyl complexes **1a** and **2a** was estimated by using the Griess reagent assay.[27–30] The presence of photolabile NO in complexes **1a** and **2a** was further confirmed by observing the increase in optical density of the produced azo dye at approximately 538 nm in ultraviolet light (λ_{max} = 365 nm). Under dark conditions, a negligible amount of NO was found to be released from both the nitrosyls. During the Griess reaction, exposure of UV light for 30 minutes to 50 μM solutions of complexes **1a** and **2a** gave rise to nearly 7 μM (Figure 4, Figure S9 in the Supporting Information, and Table 2) of produced dye. The change in the absorbance of azo dye produced from a Griess reagent was found to be very small on visible-light (100 W tungsten lamp) exposure to the same solutions. The results of estimated NO from **1a** and **2a** were compared with the data obtained from sodium nitroprusside (SNP), a well-known NO-donor drug.[1d,7b] In UV light, a 50 μM solution of SNP provided approximately 4.0 μM of nitric oxide (Table 2). These data confirmed the formation of NO in solution, and the concentration of photoreleased NO in complexes **1a** and **2a** was found to be more in comparison to the NO released by SNP.

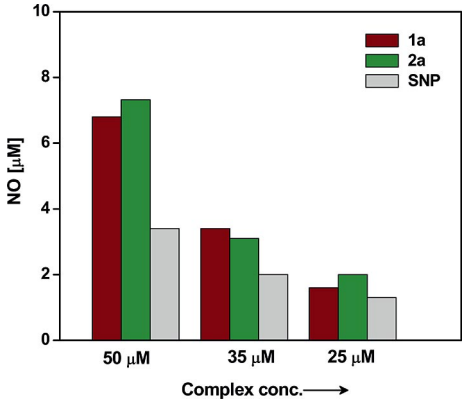

Figure 4. Bar diagrams showing the amount of photoreleased NO (dye formation) from the complexes under exposure of low-intensity UV light for 30 min.

Table 2. Determination of the amount of dye produced from the complexes **1a**, **2a**, and SNP upon reaction with Griess reagent in the dark and UV light.

	Complex conc. [μM]	Concentration of dye produced [μM][a]	
		In dark	Exposure to UV light
1a	50	0.02	6.8 ± 1.0
2a	50	0.09	7.3 ± 1.0
SNP	50	0.04	3.4 ± 0.5

[a] Average of three experiments.

DPPH Radical Quenching Studies

The antioxidant properties of several amines, phenols, natural products, and foods have been quantified by homolytic addition of DPPH radical with reactive oxygen and/or reactive nitrogen species.[31,32] During this study, its violet color turned to light yellow with a λ_{max} shift from 520 to 320 nm. We were interested to observe the disappearance of an intense violet color in the presence of photolytically cleaved NO from the nitrosyl complexes **1a** and **2a** in such a way that NO itself as well as other reactive species could decolorize the solution of DPPH radical. The solutions of nitrosyl complexes in dichloromethane were exposed to UV light in the presence of the DPPH radical, and we observed a decrease in the absorbance of DPPH with λ_{max} near 520 nm (shown in Figure S10 of the Supporting Information). The estimated amount of the generated reactive species was found to be nearly 10 and 15 μM when the solutions of **1a** and **2a** were exposed to UV light (λ_{max} = 365 nm) for an hour in the presence of the DPPH radical.

NO-Scavenging Activity of Complex $[Ru^{III}(L^1)(PPh_3)_2(Cl)]$ (1)

The use of transition-metal complexes as nitric oxide scavengers was found to be an important approach to treat NO-mediated diseases.[33] In this endeavor, the NO-scavenging ability of complexes **1** and **2** was studied by means of Griess reagent assay with a UV-visible spectrophotometer. The electronic absorption spectra were taken in the absence and in the presence of complexes. The production of nearly 23 μM of NO was detected when 25 μM aqueous solution of sodium nitrite was prepared in a 1 mL cuvette with 100 μL of the Griess reagent. The presence of a 50 μM concentration of complex **1** in the same cuvette lowered the concentration of produced NO from 23 to 17 μM, and the scavenging of nearly 6 μM of NO was observed (Figure 5). However, complex **2** was not found to be a good scavenger of NO, even at a very high concentration.

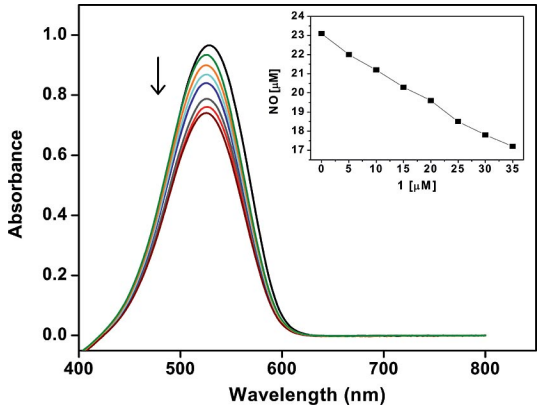

Figure 5. Electronic spectra showing scavenging of NO in the presence of different concentrations of complex **1** (0–35 μM) in the Griess assay (Griess reagent and sodium nitrite). Inset: Changes in the amount of dye formation with different concentrations of complex **1** in the presence of Griess reagent.

Density Functional Theory (DFT) Calculations

DFT calculations for free cation (without counteranion) of complex **2a** were performed at the B3LYP level[21,34] using the LANL2DZ basis set for the ruthenium center and the 6-31G(d) basis set[34,35] for non-metal atoms (C, H, N, O, P, and Cl). The structural data obtained from the optimized geometry of **2a** agrees quite well with experimental (X-ray) results, whereas the Ru–N_{NO} (1.782 Å) and N–O (1.188 Å) bond lengths in the computed structure were found to be slightly longer (shown in Table 1). The Ru–N_{NO} and N–O bond lengths along with the Ru–N–O angle (178.61°) exhibited the presence of $\{Ru–NO\}^6$ species in the optimized geometry of **2a**. The nitrosyl (ν_{NO}) stretching frequency (ca. 1813 cm^{-1}) in the optimized geometry deviates from the experimental value by nearly 4% when using the LANL2DZ basis set. The HOMO was found to be located predominantly over the metal center. The frontier molecular orbitals for complex **2a** are shown in Figure S11 in the Supporting Information.

The time-dependent DFT calculations were also performed to evaluate the electronic absorption spectrum of complex **2a** (Figure S12 in the Supporting Information). The absorption bands, found in the computed spectrum were closely related to that of the bands in the experimental spectrum. The electronic transitions, excitation energies [eV], and oscillator strengths (*f*) obtained from TD-DFT are displayed in Table S1 of the Supporting Information. The absorption peak calculated at 327 nm was slightly redshifted relative to the experimental band (at 320 nm) and probably arises from HOMO→LUMO+5, HOMO→LUMO+3, and HOMO–2→LUMO+3 transitions. A band near 297 nm was also redshifted relative to the experimental band (at 276 nm) and appears to be a composition of three main transitions dominated by HOMO–13→LUMO+3, HOMO–18→LUMO, and HOMO–14→LUMO+3 excitations.

Conclusion

In conclusion, two nitric oxide (NO)-donating complexes, $[Ru(L^1)(PPh_3)_2(NO)](ClO_4)$ (**1a**) and $[Ru(L^2)(PPh_3)_2(NO)](ClO_4)$ (**2a**), were derived from the ligands that contained two carboxylate groups. Both the complexes were found to be diamagnetic and to have $\{RuNO\}^6$ moieties with $S = 0$ ground state. These complexes were characterized by ^1H and ^{31}P NMR spectral studies, the results of which were also supported by ESI-MS data. The crystal structure of **2a** was authenticated by using X-ray crystallography. Coordinated NO in complexes **1a** and **2a** was found to be photolabile under visible light as well as in UV light. The amount of this NO was estimated using the Griess reagent assay. The measurement of quantum yields for NO photorelease was also performed for **1a** and **2a**. A DPPH radical quenching assay was performed under aerobic conditions to detect the amount of generated reactive nitrogen species and/or reactive oxygen species during photolysis of NO from nitrosyl complexes.

Experimental Section

Reagents and Materials: All the solvents used were of reagent grade. Analytical-grade reagents of sodium nitrite, iminodiacetic acid (Sigma Aldrich, Steinheim, Germany), $RuCl_3·3H_2O$, triphenylphosphine (SRL, Mumbai, India), anhydrous disodium hydrogen phosphate, pyridine 2,6-dicarboxylic acid (RFCL Ltd. New Delhi, India), sodium dihydrogen phosphate (Chemport India Pvt. Ltd. Mumbai, India), sodium perchlorate monohydrate, sulfanilamide, and naphthylethylenediamine dihydrochloride (NED) (Himedia Laboratories Pvt. Ltd., Mumbai, India) were used as obtained. Double-distilled water was used in all the experiments.

Physical Measurements: Infrared spectra were obtained as KBr pellets with a Thermo Nicolet Nexus FTIR spectrometer, using 16 scans and were reported in cm^{-1}. Electronic absorption spectra were recorded in dichloromethane and methanol with an Evolution 600 Thermo Scientific UV/Vis spectrophotometer. ^1H and ^{31}P NMR spectra were recorded with a Bruker Avance (500.13 MHz) spectrometer in the deuterated solvents. The ESI-MS of the sam-

ples (a solution of methanol was used) were recorded in the positive-ion mode with a Thermo Finnigan LCQ Deca mass spectrometer.

$[Ru^{III}(L^1)(PPh_3)_2(Cl)]$ (1): A batch of iminodiacetic acid (0.02 g, 0.15 mmol; L^1H_2, in which H stands for dissociable protons) with ethanol (15 mL) was added directly to a solution of $[Ru(PPh_3)_3Cl_2]$ (0.096 g, 0.1 mmol) in benzene (15 mL). This mixture was heated to reflux for 5–6 h. The color of the solution changed from brown to orange red. The mixture was cooled to room temperature and was filtered. The filtrate was kept for 2 days to obtain a precipitate of complex **1**, which was washed with cold ethanol and diethyl ether and then dried, yield 65%. $C_{40}H_{35}ClNO_4P_2Ru$ (792.18): calcd. C 60.65, H 4.45, N 1.77; found C 59.88, H 4.51, N 1.72. IR (KBr disk): $\tilde{\nu}$ = 1654 (ν_{CO}), 1598, 1480, 1440, 1102, 748, 741, 696, 522 (ν_{PPh_3}) cm^{-1}. UV/Vis (MeOH): λ_{max} (ε, $M^{-1}cm^{-1}$) = 373 (11400), 458 (6384) nm.

$[Ru^{III}(L^2)(PPh_3)_2(Cl)]$ (2): Complex **2** was synthesized from the reaction of $[Ru(PPh_3)_3Cl_2]$ with pyridine-2,6-dicarboxylic acid (L^2H_2, in which H stands for dissociable protons) in 1:1 equivalents in ethanol following the method reported earlier.[11] Yield: 62%. $C_{43}H_{33}ClNO_4P_2Ru$ (826.20): calcd. C 62.51, H 4.03, N 1.70; found C 61.99, H 4.11, N 1.61. IR (KBr disk): $\tilde{\nu}$ = 1648 (ν_{CO}), 1607, 1481, 1432, 1349, 1315, 1264, 1091, 750, 697, 520 (ν_{PPh_3}) cm^{-1}. UV/Vis (MeOH): λ_{max} (ε, $M^{-1}cm^{-1}$) = 261 (12727), 396 (5454) nm.

$[Ru(L^1)(PPh_3)_2(NO)](ClO_4)$ (1a): $NaNO_2$ (0.070 g, 1 mmol) was added to a warm solution of complex **1** (0.08 g, 0.1 mmol) with methanol (20 mL). The mixture was heated under reflux conditions for 30 min. The color of the solution turned from brown red to yellow. Then perchloric acid (0.5 mL of $HClO_4$) was added to the same solution. The mixture was filtered and was kept for 2–3 d to obtain a precipitate of complex **1a**, yield 54%. $C_{40}H_{35}ClN_2O_9P_2Ru$ (886.18): calcd. C 54.21, H 3.98, N 3.16; found C 53.98, H 4.01, N 3.22. ESI-MS: *m*/*z* = 786.9 $[Ru(L^1)(PPh_3)_2(NO)]^+$. IR (KBr disk): $\tilde{\nu}$ = 1880 (ν_{NO}), 1695, 1671 (ν_{CO}), 1485, 1440, 1345, 1257, 1095, 622 (ν_{ClO_4}), 745, 694, 518 (ν_{PPh_3}) cm^{-1}. UV/Vis (CH_2Cl_2): λ_{max} (ε, $M^{-1}cm^{-1}$) = 282 (25440) nm. ^1H NMR [$(CD_3)_2SO$, 500 MHz]: δ = 7.41–7.35 (m, 18 H), 7.28–7.23 (m, 12 H), 3.38 (s, 4 H) ppm. ^{31}P NMR [$(CD_3)_2SO$, 500 MHz]: δ = 20.20 ppm.

$[Ru(L^2)(PPh_3)_2(NO)](ClO_4)$ (2a): A batch of complex **2** (0.025 g, 0.03 mmol) was dissolved in dichloromethane (30 mL) to obtain a brown-red solution in a 100 mL round-bottom flask. Then acidified distilled water (25 mL) was layered over this solution. Sodium nitrite (0.3 g, 4.3 mmol) was added to the bilayer solution, and the mixture was stirred at room temperature for 1–1.5 h to obtain a yellow solution of complex **2a**. The dichloromethane layer was separated out, and $NaClO_4$ (in an excess amount) with methanol (5 mL) was added to this solution. Stirring of this solution was continued for another 1 h. The solvent mixture was evaporated immediately to obtain a yellow solid. To remove the excess amount of $NaClO_4$, this solid was further dissolved in dichloromethane (10 mL) and was removed by filtration. Then hexane (10 mL) was added to the filtrate to obtain a yellow precipitate of complex **2a** (0.016 g, 0.017 mmol), yield 56.66%. $C_{44}H_{35}Cl_3N_2O_9P_2Ru$ (1003.99): calcd. C 52.58, H 3.51, N 2.79; found C 52.88, H 3.20, N 2.56. ESI-MS: *m*/*z* = 820.99 $[Ru(L^2)(PPh_3)_2(NO)]^+$, 558.13 $[Ru(L^2)(PPh_3)(NO)]^+$. IR (KBr disk): $\tilde{\nu}$ = 1895 (ν_{NO}), 1693 (ν_{CO}), 1630, 1482, 1433, 1380, 1315, 1252, 1090, 624 (ν_{ClO_4}), 745, 696, 517 (ν_{PPh_3}) cm^{-1}. UV/Vis (CH_3CN): λ_{max} (ε, $M^{-1}cm^{-1}$) = 280 (20375), 321 (23125) nm. ^1H NMR (CD_3CN, 500 MHz): δ = 8.22 (dd, 1 H), 7.72–7.65 (m, 6 H), 7.63 (d, 2 H), 7.58–7.50 (m, 12 H), 7.29–7.20 (m, 12 H) ppm. ^{31}P NMR (CD_3CN, 500 MHz): δ = 19.67 ppm.

Griess Reagent Assay: The amount of NO produced from complexes **1a** and **2a** was estimated using the Griess reagent (GR) assay.[27–30] It was freshly prepared by mixing equal volumes of 1% sulfanilamide in 5% orthophosphoric acid and 0.1% naphthylethylenediamine dihydrochloride (NED) in distilled water. To estimate the production of NO or nitrite ion, the absorbance near 538 nm owing to the formation of azo dye was measured. Aqueous solutions of $NaNO_2$ with different concentrations (5–50 μM) were used to prepare a standard curve for the determination of nitrite.[27]

X-ray Crystallography: Single crystals of complex **2a** were grown by layering hexane over the solution of complex in a mixture of CH_2Cl_2/methanol; crystal data and data-collection parameters are shown in Table 3. The diffraction data for **2a** was collected at 293 K with a Bruker Kappa Apex-II CCD diffractometer by using graphite-monochromated Mo-K_α radiation (λ = 0.71073 Å). The structure was solved and refined by full-matrix least-squares techniques on F^2 using the SHELXTL program.[36,37] The absorption corrections were performed by the multiscan technique. The anisotropic thermal parameters were refined for all of the non-hydrogen atoms. Hydrogen atoms were refined in riding model approximations with a common isotropic displacement parameter. X-ray analysis revealed the presence of three molecules of **2a** and three dichloromethane molecules as the solvent of crystallization in one unit cell. Hydrogen atoms were placed in geometrically calculated positions and refined using a riding model. Images were created with the DIAMOND program.[38]

Table 3. Summary of crystal data and data-collection parameters for **2a**·CH_2Cl_2.

Empirical formula	$C_{44}H_{35}Cl_3N_2O_9P_2Ru$
M_r [g mol^{-1}]	1005.10
Space group	$P\bar{1}$
T [K]	293(2)
λ [Å] (Mo-K_α)	0.71073
Crystal system	triclinic
a [Å]	15.653(5)
b [Å]	16.927(5)
c [Å]	25.150(5)
α [°]	95.497 (5)
β [°]	92.449(5)
γ [°]	93.807(5)
V [Å^3]	6610(3)
Z	6
$\rho_{calcd.}$ [g cm^{-3}]	1.515
Crystal size [mm]	0.28 × 0.24 × 0.21
F(000)	3060.0
θ range for data collection	0.81–28.39
Index ranges	$-20 < h < 20$, $-22 < k < 13$, $-33 < l < 33$
Refinement method	full-matrix least squares on F^2
Data/restraints/parameters	33151/0/1648
GoF[a] on F^2	1.012
$R1$[b] [$I > 2\sigma(I)$]	0.0550
$R1$[all data]	0.1078
$wR2$[c] [$I > 2\sigma(I)$]	0.1461
$wR2$ [all data]	0.1879

[a] GOF = $\{\Sigma[w(F_o^2 - F_c^2)^2]/M - N\}^{1/2}$ (M = number of reflections, N = number of parameters refined). [b] $R1 = \Sigma|F_o| - |F_c|/\Sigma|F_o|$. [c] $wR2 = \{\Sigma[w(F_o^2 - F_c^2)^2]/\Sigma[(F_o^2)^2]\}^{1/2}$.

CCDC-946749 (for **2a**) contains the supplementary crystallographic data for this paper. These data can be obtained free of charge from The Cambridge Crystallographic Data Centre via www.ccdc.cam.ac.uk/data_request/cif.

Quantum Yield Measurements: Quantum yields were determined by actinometry studies using a ferric oxalate solution. The intensity of the UV light (λ_{irr} = 365 nm) was determined with a ferrioxalate actinometer (0.006 M solution of potassium ferrioxalate in 0.1 N H_2SO_4).[39–43] Quantum yields (ϕ) of NO photorelease for complexes **1a** and **2a** were determined by the decrease in their absorption bands near 282 and 321 nm, respectively, when irradiated with 365 nm light and were calculated by following the procedure reported earlier.[42]

Computational Study Using DFT: DFT calculations were carried out using the B3LYP exchange correlation functional[21,34] and implemented in the Gaussian 03 program package.[34,35,44,45] The electronic structure of the complex was determined using the LANL2DZ basis set[35] for the ruthenium center and the 6-31G(d) basis set[34,35] for other nonmetal atoms. The X-ray coordinates of complex **2a** were used as input data for geometry optimization. The GaussView 4 program was used for pictorial representation of frontier molecular orbitals.

Supporting Information (see footnote on the first page of this article): Characterization of complexes by IR, UV/Vis, NMR spectroscopy, and ESI-MS spectral studies.

Acknowledgments

K. G. is thankful to the Council of Scientific and Industrial Research (CSIR), India for financial assistance [grant number 01(2720)/13/EMR-II]. S. K. and R. K. are also thankful to the CSIR for financial support.

[1] a) L. J. Ignarro, *Nitric Oxide: Biology and Pathobiology*, 2nd ed., Academic Press, San Diego, CA, **2000**; b) G. B. Richter-Addo, P. Legzdins, J. Burstyn, *Chem. Rev.* **2002**, *102*, 857–859; c) K. Bian, M. F. Doursout, F. Murad, *J. Clin. Hypertens.* **2008**, *10*, 304–310; d) M. J. Rose, P. K. Mascharak, *Coord. Chem. Rev.* **2008**, *252*, 2093–2114; e) P. C. Ford, I. M. Lorkovic, *Chem. Rev.* **2002**, *102*, 993–1018; f) M. J. Rose, P. K. Mascharak, *Curr. Opin. Chem. Biol.* **2008**, *12*, 238–244.
[2] D. E. Koshland, *Science* **1992**, *258*, 1861.
[3] S. Kalsner (Ed.), *Nitric Oxide Free Radicals in Peripheral Neurotransmission*, Birkhauser, Boston, **2000**.
[4] S. Moncada, E. A. Higgs, G. Bagetta (Eds.), *Nitric Oxide & the Cell: Proliferation, Differentiation and Death*, Portland Press, London, **1998**.
[5] a) G. B. Richter-Addo, P. Legzdins, *Metal Nitrosyls*, Oxford University Press, New York, **1992**; b) G. B. Richter-Addo, P. Legzdins, J. Burstyn, *Chem. Rev.* **2002**, *102*, 857–859.
[6] a) P. C. Ford, *Inorg. Chem.* **2010**, *49*, 6226–6239; b) P. C. Ford, *Acc. Chem. Res.* **2008**, *41*, 190–200; c) P. C. Ford, B. O. Fernandez, M. D. Lim, *Chem. Rev.* **2005**, *105*, 2439–2455.
[7] a) N. L. Fry, P. K. Mascharak, *Acc. Chem. Res.* **2011**, *44*, 289–298; b) A. A. Eroy-Reveles, Y. Leung, C. M. Beavers, M. M. Olmstead, P. K. Mascharak, *J. Am. Chem. Soc.* **2008**, *130*, 4447–4458; c) R. K. Afshar, A. K. Patra, M. M. Olmstead, P. K. Mascharak, *Inorg. Chem.* **2004**, *43*, 5736–5743; d) A. K. Patra, M. J. Rose, K. A. Murphy, M. M. Olmstead, P. K. Mascharak, *Inorg. Chem.* **2004**, *43*, 4487–4495; e) M. J. Rose, M. M. Olmstead, P. K. Mascharak, *J. Am. Chem. Soc.* **2007**, *129*, 5342–5343; f) G. M. Halpenny, P. K. Mascharak, *Inorg. Chem.* **2009**, *48*, 1490–1497.
[8] a) M. G. Sauaia, R. G. de Lima, A. C. Tedesco, R. S. da Silva, *Inorg. Chem.* **2005**, *44*, 9946–9951; b) M. G. Sauaia, R. G. de Lima, A. C. Tedesco, R. S. da Silva, *J. Am. Chem. Soc.* **2003**, *125*, 14718–14719.
[9] a) G. K. Lahiri, W. Kaim, *Dalton Trans.* **2010**, *39*, 4471–4478; b) S. Maji, B. Sarkar, M. Patra, A. K. Das, S. M. Mobin, W. Kaim, G. K. Lahiri, *Inorg. Chem.* **2008**, *47*, 3218–3227; c) N. Chanda, D. Paul, S. Kar, S. M. Mobin, A. Datta, V. G. Puranik, K. K. Rao, G. K. Lahiri, *Inorg. Chem.* **2005**, *44*, 3499–3511; d) N. Chanda, S. M. Mobin, V. G. Puranik, A. Datta, M. Niemeyer, G. K. Lahiri, *Inorg. Chem.* **2004**, *43*, 1056–1064.
[10] a) K. Ghosh, S. Kumar, R. Kumar, U. P. Singh, *Eur. J. Inorg. Chem.* **2012**, 929–938; b) K. Ghosh, S. Kumar, R. Kumar, U. P. Singh, N. Goel, *Organometallics* **2011**, *30*, 2498–2505; c) K. Ghosh, S. Kumar, R. Kumar, U. P. Singh, N. Goel, *Inorg. Chem.* **2010**, *49*, 7235–7237.
[11] K. Ghosh, S. Kumar, R. Kumar, *Inorg. Chem. Commun.* **2011**, *14*, 146–149.
[12] K. Ghosh, R. Kumar, S. Kumar, J. S. Meena, *Dalton Trans.* **2013**, *42*, 13444–13452.
[13] K. Ghosh, S. Kumar, R. Kumar, *Inorg. Chim. Acta* **2013**, *405*, 24–30.
[14] a) M. M. T. Khan, D. Chatterjee, R. R. Merchant, P. Paul, S. H. R. Abdi, D. Srinivas, M. R. H. Siddiqui, M. A. Moiz, M. M. Bhadbhade, K. Venkatasubramanian, *Inorg. Chem.* **1992**, *31*, 2711–2718; b) A. Das, T. Scherer, S. Maji, T. K. Mondal, S. M. Mobin, F. A. Urbanos, R. Jimenez-Aparicio, W. Kaim, G. K. Lahiri, *Inorg. Chem.* **2011**, *50*, 7040–7049.
[15] G. K. Lahiri, S. Bhattacharya, M. Mukherjee, A. K. Mukherjee, A. Chakravorty, *Inorg. Chem.* **1987**, *26*, 3359–3365.
[16] R. Raveendran, S. Pal, *J. Organomet. Chem.* **2007**, *692*, 824–830.
[17] B. Birkmann, B. T. Owens, S. Bandyopadhyay, G. Wu, P. C. Ford, *J. Inorg. Biochem.* **2009**, *103*, 237–242.
[18] a) S. Sarkar, B. Sarkar, N. Chanda, S. Kar, S. M. Mobin, J. Fiedler, W. Kaim, G. K. Lahiri, *Inorg. Chem.* **2005**, *44*, 6092–6099; b) P. De, B. Sarkar, S. Maji, A. K. Das, E. Bulak, S. M. Mobin, W. Kaim, G. K. Lahiri, *Eur. J. Inorg. Chem.* **2009**, 2702–2710.
[19] a) G. R. Desiraju, T. Steiner, *The Weak Hydrogen Bond in Structural Chemistry and Biology*, Oxford University Press, New York, **1999**; b) A. Nangia, *J. Chem. Sci.* **2010**, *122*, 295–310; c) R. R. Knowles, E. N. Jacobsen, *Proc. Natl. Acad. Sci. USA* **2010**, *107*, 20678–20685.
[20] D. Sukanya, R. Prabhakaran, K. Natarajan, *Polyhedron* **2006**, *25*, 2223–2228.
[21] K. Karidi, A. Garoufis, A. Tsipis, N. Hadjiliadis, H. den Dulk, J. Reedijk, *Dalton Trans.* **2005**, 1176–1187.
[22] J. H. Enemark, R. D. Feltham, *Coord. Chem. Rev.* **1974**, *13*, 339–406.
[23] R. Raveendran, S. Pal, *J. Organomet. Chem.* **2009**, *694*, 1482–1486.
[24] P. Munshi, R. Samanta, G. K. Lahiri, *J. Organomet. Chem.* **1999**, *586*, 176–183.
[25] R. Raveendran, S. Pal, *Inorg. Chim. Acta* **2006**, *359*, 3212–3220.
[26] B. P. Sullivan, J. M. Calvert, T. J. Meyer, *Inorg. Chem.* **1980**, *19*, 1404–1407.
[27] D. Tsikas, *J. Chromatogr. B* **2007**, *851*, 51–70.
[28] S. Sharma, S. K. Kulkarni, J. N. Agrewala, K. Chopra, *Eur. J. Pharmacol.* **2006**, *536*, 256–261.
[29] A. Chakraborty, N. Gupta, K. Ghosh, P. Roy, *Toxicol. in vitro* **2010**, *24*, 1215–1228.
[30] D. Sharma, P. Goyal, A. Singh, S. S. Trivedi, J. Bhattacharjee, *Anatol. J. Obstet. Gynecol.* **2010**, 1.
[31] P. Ionita, *Chem. Pap.* **2005**, *59*, 11–16.
[32] a) H.-M. Kang, M. E. Saltveit, *J. Agric. Food Chem.* **2002**, *50*, 513–518; b) A. Chandrasekara, F. Shahidi, *J. Agric. Food Chem.* **2011**, *59*, 428–436; c) M. C. Foti, C. Daquino, C. Geraci, *J. Org. Chem.* **2004**, *69*, 2309–2314; d) H. Aoshima, H. Tsunoue, H. Koda, Y. Kiso, *J. Agric. Food Chem.* **2004**, *52*, 5240–5244.
[33] a) B. R. Cameron, M. C. Darkes, H. Yee, M. Olsen, S. P. Fricker, R. T. Skerlj, G. J. Bridger, N. A. Davies, M. T. Wilson, D. J. Rose, J. Zubieta, *Inorg. Chem.* **2003**, *42*, 1868–1876; b) B. R. Cameron, M. C. Darkes, I. R. Baird, R. T. Skerlj, Z. L. Suntucci, S. P. Fricker, *Inorg. Chem.* **2003**, *42*, 4102–4108.

[34] P. De, S. Maji, A. D. Chowdhury, S. M. Mobin, T. K. Mondal, A. Paretzki, G. K. Lahiri, *Dalton Trans.* **2011**, *40*, 12527–12539.
[35] a) F. Roncaroli, M. E. Ruggiero, D. W. Franco, G. L. Estiu, J. A. Olabe, *Inorg. Chem.* **2002**, *41*, 5760–5769; b) M. Videla, J. S. Jacinto, R. Baggio, M. T. Garland, P. Singh, W. Kaim, L. D. Slep, J. A. Olabe, *Inorg. Chem.* **2006**, *45*, 8608–8617.
[36] G. M. Sheldrick, *Acta Crystallogr., Sect. A* **1990**, *46*, 467–473.
[37] G. M. Sheldrick, *SHELXTL-NT 2000*, version 6.12, *Reference Manual*, University of Göttingen, Germany, Pergamon, New York, **1980**.
[38] B. Klaus, *DIAMOND*, version 1.2c, University of Bonn, Germany, **1999**.
[39] C. F. Works, C. J. Jocher, G. D. Bart, X. Bu, P. C. Ford, *Inorg. Chem.* **2002**, *41*, 3728–3739.
[40] J. Lee, J. Kim, W. Choi, *Environ. Sci. Technol.* **2007**, *41*, 5433–5438.
[41] H. J. Kuhn, S. E. Braslavsky, R. Schmidt, *Pure Appl. Chem.* **1989**, *61*, 187–210.
[42] S. K. Nayak, G. J. Farrell, T. J. Burkey, *Inorg. Chem.* **1994**, *33*, 2236–2242.
[43] M. G. Sauaia, F. de S. Oliveira, A. C. Tedesco, R. S. da Silva, *Inorg. Chim. Acta* **2003**, *355*, 191–196.
[44] M. J. Frisch, G. W. Trucks, H. B. Schlegel, G. E. Scuseria, M. A. Robb, J. R. Cheeseman, J. A. Montgomery Jr., T. Vreven, K. N. Kudin, J. C. Burant, J. M. Millam, S. S. Iyengar, J. Tomasi, V. Barone, B. Mennucci, M. Cossi, G. Scalmani, N. Rega, G. A. Petersson, H. Nakatsuji, M. Hada, M. Ehara, K. Toyota, R. Fukuda, J. Hasegawa, M. Ishida, T. Nakajima, Y. Honda, O. Kitao, H. Nakai, M. Klene, X. Li, J. E. Knox, H. P. Hratchian, J. B. Cross, C. Adamo, J. Jaramillo, R. Gomperts, R. E. Stratmann, O. Yazyev, A. J. Austin, R. Cammi, C. Pomelli, J. W. Ochterski, P. Y. Ayala, K. Morokuma, G. A. Voth, P. Salvador, J. J. Dannenberg, V. G. Zakrzewski, S. Dapprich, A. D. Daniels, M. C. Strain, O. Farkas, D. K. Malick, A. D. Rabuck, K. Raghavachari, J. B. Foresman, J. V. Ortiz, Q. Cui, A. G. Baboul, S. Clifford, J. Cioslowski, B. B. Stefanov, G. Liu, A. Liashenko, P. Piskorz, I. Komaromi, R. L. Martin, D. J. Fox, T. Keith, M. A. Al-Laham, C. Y. Peng, A. Nanayakkara, M. Challacombe, P. M. W. Gill, B. Johnson, W. Chen, M. W. Wong, C. Gonzalez, J. A. Pople, *Gaussian 03*, revision E.01, Gaussian, Inc., Pittsburgh, PA, **2007**.
[45] a) A. D. Becke, *J. Chem. Phys.* **1992**, *96*, 2155–2160; b) A. D. Becke, *J. Chem. Phys.* **1993**, *98*, 5648–5652.

Received: September 19, 2013
Published Online: February 20, 2014

